

Final Report 2007

PHYSICS-BASED SIMULATION OF EARTHQUAKE OCCURRENCE IN FAULT SYSTEMS

Principal investigator: James H. Dieterich
Department of Earth Sciences
University of California, Riverside

Introduction

This project began in 2005. Postdoctoral researcher Keith Richards-Dinger joined the project in 2006. Project goals were to develop a large-scale 3D physics-based earthquake simulator for a) investigation of earthquake processes in geometrically complex fault systems, and b) use with the SCEC community fault model to simulate of earthquake occurrence and deformation in southern California, and to evaluate earthquake probabilities.

To address these goals the simulator is

- 1) flexible to incorporate alternative models of earthquake source processes and input parameters;
- 2) capable of modeling earthquake occurrence over a large range of length and time scales to permit comparisons with earthquake catalogs and paleoseismology data;
- 3) fully three-dimensional to properly represent fault interactions and to permit comparisons with deformation observations;
- 4) able to model time-dependent fault interactions, as well as foreshocks and aftershocks, by incorporating time-dependent earthquake nucleation inherent to rate- and state-dependent friction; and
- 5) suitable for implementation with complex fault system geometry, including the SCEC community fault model at a resolution appropriate to items 1) through 4).

A long-term objective is to implement the SCEC community fault model at a 1km^2 resolution, to permit comparisons with the southern California instrumental catalog data at a minimum earthquake magnitude threshold of about $M3.5$. This requires simulations of at least 10^5 events

Overview of Modeling Approach

Simulations of synthetic catalogs of 10^5 or more earthquakes, based on detailed fully dynamical deterministic calculations of each earthquake rupture, remain far out of reach with current computational technology. To achieve sufficient computational efficiency, this project employs physically reasonable large-scale approximations and simplifications of the earthquake generation process, together with efficient numerical schema.

A boundary element method, developed by Dieterich (1995) for simulations with single planar faults, was successfully adapted and generalized for simulation of earthquakes on a 3D system of explicitly modeled faults. This quasi-dynamical approach approximates the gross dynamics of the earthquake source, and it incorporates fault aging and nucleation processes implicit to rate- and state-dependent friction. The use of rate-state friction enables modeling of clustering phenomena including foreshocks and aftershocks. Additional efficiencies are obtained by a) use of a computational approach that avoids solution of systems of simultaneous equations, and b) use of event-driven computational steps, instead of time stepping at closely spaced intervals. In the model, fault segments may be at one of three sliding states. The sliding states correspond to a fully locked condition with time dependent strengthening (state 0), an incipient slip condition with time- and stress-dependent nucleation of unstable slip (state 1), and seismic slip at speeds

controlled by the dynamic shear impedance criteria and together with dynamic stress drop (state 2). Computational events, which update stressing conditions, occur at the transitions between states.

Results

Program design and implementation. A large-scale simulation code was successfully implemented, and has undergone preliminary tests. The model incorporates generalized 3D interactions among fault segments with different orientations and modes of slip, together with rate- and state-dependent fault properties, including nucleation processes. Stress interactions employ the Okada (1992) solutions for rectangular dislocation elements.

Nucleation with variable normal and shear stress. The original planar-fault simulator employed analytic solutions to represent rate- and state-dependent nucleation processes (state 1) under conditions of constant normal stress. However, both shear and normal stresses vary in geometrically complex fault-systems. To enable use of computationally efficient analytic solutions with full coupling of fault friction to varying shear and normal stress, we have derived a generalized form of the Dieterich (1992) earthquake nucleation solution for use with Coulomb stressing. Under conditions where nucleation is in progress ($\theta \gg D_c / \dot{\delta}$), the local acceleration of slip at a fault element is given by

$$d\omega = \frac{-1}{A\sigma} [Cdt + \omega dS] , \quad (1)$$

where slip speed $\dot{\delta} = 1/\omega$, C is a constant term containing model and constitutive parameters, σ is local fault normal stress, and A is the rate constant in the rate- and state-dependent friction formulation. S is a modified Coulomb stress function

$$dS = d\tau - \mu' d\sigma \quad \text{with} \quad \mu' = \mu - \alpha , \quad (2)$$

where μ is the nominal coefficient of friction during state 1 slip, α is a material parameter ($0 \leq \alpha \leq \mu$) governing the effect of normal stress on evolution of friction. Analytic solutions of (3) are easily obtained for the evolution of slip speed and time to instability at constant \dot{S} . This formulation will also be of general use for investigations of earthquake nucleation processes.

Computational efficiency. Tests of the code confirm our initial estimates for the scaling of computation time with model size (number of fault elements) and number of earthquakes. The model is very efficient. Computation times required to set up the interaction matrix for a model fault geometry scale by N^2 , whereas computation times to execute simulations scale by about N^1 , where N is the number of fault elements. Simulations of 50,000 events in models with 1500 require about 15 minutes on a single 2.5 GHz G5 processor – this benchmark gives projected computation times of about 19 hours for simulations of 100,000 events in models with 30,000 elements. Test calculations with 10,000 elements confirm this scaling. Setup time for the model interaction matrix with 30,000 elements will require about 10 hours, but this operation needs to be done just once for a specific fault geometry.

Preliminary modeling results. Figures 1 – 4 summarize some initial results and examples of computations obtained with the model. Figure 1 illustrates characteristics of rupture propagation in a M8 earthquake along a planar strike-slip fault made up of 10,000 fault elements. As found previously by Dieterich (1995) rupture propagation and slip is typically pulse-like in simulations

with heterogeneous fault stresses, inherited from prior slip events. That is, earthquake slip occurs primarily within a narrow band immediately behind the rupture front. The large-scale simulations show additional complexity behind the rupture front that is characterized by weak backward propagating zones of reactivated slip. Rupture propagation and slip of faults with homogeneous stresses are more crack-like in character with continuing slip over much, or all, of the fault surface after the rupture front passes. In all simulations reported here, input parameters were set for average dynamic stress drops (in large events) and slip speeds of 5 MPa and 1 m/s respectively, with an implicit shear wave speed of 3 km/sec. Rupture propagation speeds in these simulations usually fall in the range 2.0-2.4 km/sec.

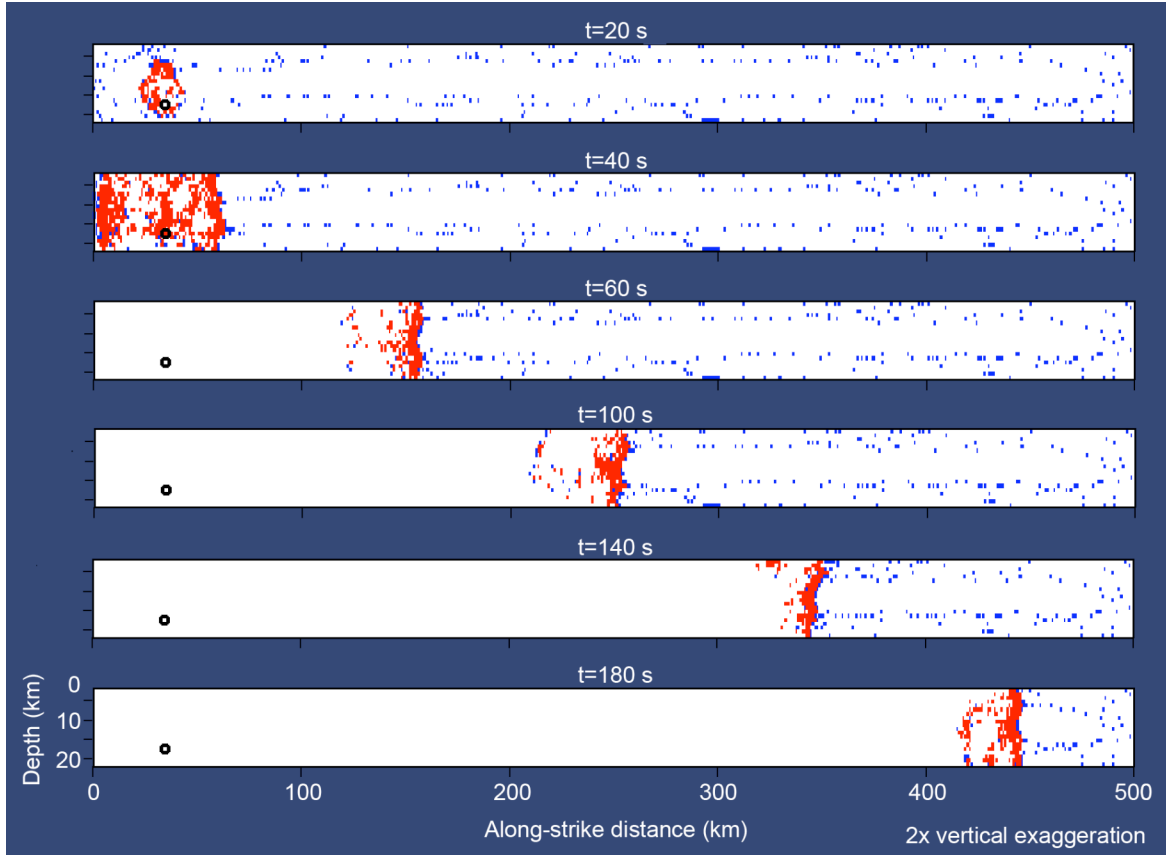


Figure 1. Rupture propagation sequence for a M~8 earthquake in which the entire fault slipped. The model is a planar left-lateral strike-slip fault made up of 10^4 fault elements. Fault elements are color-coded to indicate slip state. White = state 0 (locked fault), blue = state 1 (nucleating with time- and stress rate-dependent weakening), red = state 2 (seismic slip).

A fundamental objective of this effort is to simulate earthquake interactions in geometrically complex fault systems, wherein shear and normal stress vary simultaneously during slip and couple to fault strength and sliding resistance. Figure 3 illustrates a M7.1 earthquake that occurred during a simulation of 50,000 events on a fault with random fractal roughness. The random fractal fault simulations incorporate shear and normal stress interactions at all length scales with full coupling to fault strength, nucleation processes, and sliding resistance. The somewhat patchy slip seen in the simulation shown in Figure 3 appears to be characteristic of the fractal faults, and is reminiscent of inverse solutions for earthquake sources. With the fractal faults, restraining bends fail preferentially in the largest earthquakes. Conversely, smaller earthquakes occur preferentially along releasing bends.

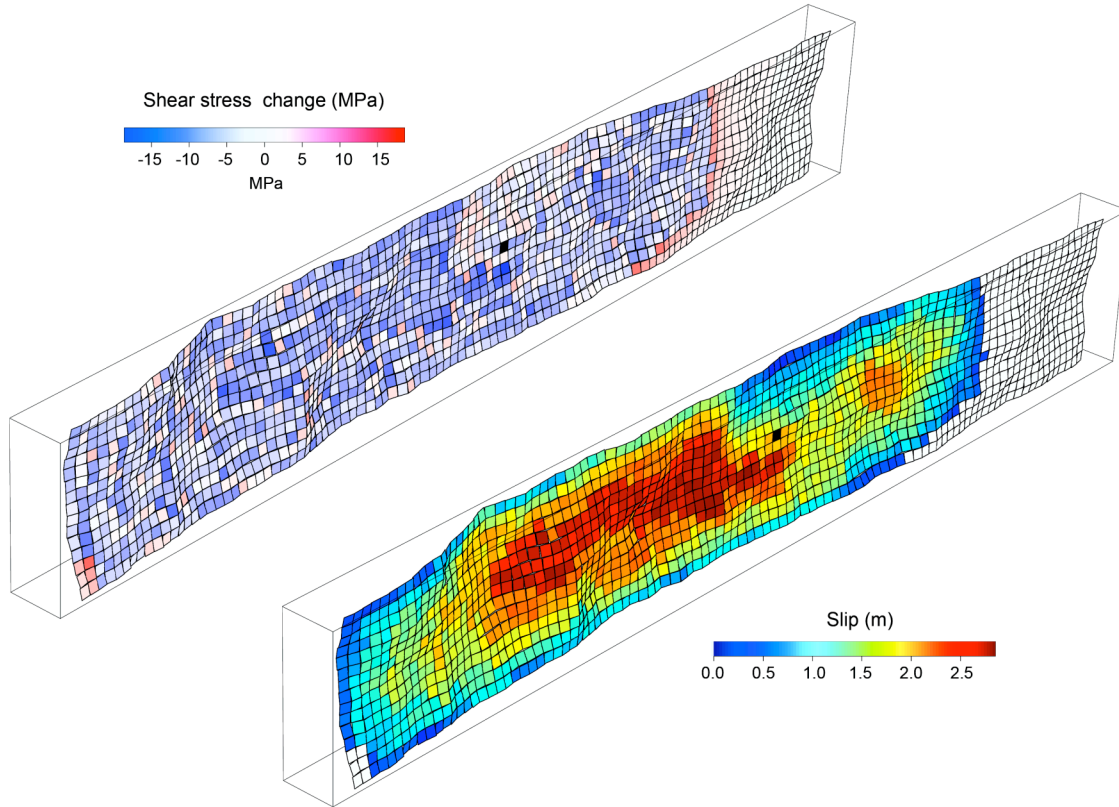


Figure 2. Slip and shear stress change for simulated M7.1 event on a fault with fractal fault roughness. Model is for strike-slip faulting (left-lateral) with 1,500 fault elements. This event was taken from a simulation with 50,000 earthquakes M3.5-M7.2. Nucleation occurred at the black element.

Thus far tests with multiple faults have been restricted to simple geometries with a single step-over. Figure 3 illustrates slip occurring in earthquakes $M \geq 6.0$ in a simulation with a 200m compressional step-over between two faults. In this, and other simulations, earthquakes $M \leq 6.0$ have a Gutenberg-Richter type magnitude-frequency distribution, while the larger earthquakes tend to grow to rupture an entire segment, resulting in a narrow peak in the distribution of large magnitude earthquakes. The segment-rupturing events are quasi-periodic while the smaller earthquakes are highly clustered. In the two-segment model of Figure 2 the small compressional step-over slightly inhibited rupture propagation between segments, giving rise to several paired events of similar magnitudes. The intervals separating the event pairs varied from 3 seconds to 0.8 years. These delayed instabilities arise from the time- and stress-dependent state-1 rupture initiation criteria, which are based on rate-state friction. The numbers of aftershocks occurring between the event pairs is indicated in red typeface in Figure 3.

This model produces highly clustered seismicity that includes foreshocks, abundant aftershocks and paired events. Previously (Dieterich, 1995) it was shown that clustering statistics in the simulations could be adjusted to match catalog statistics through adjustment of the rate-state friction parameter A and normal stress σ . Aftershocks follow Omori's decay law. Figure 4 compares clustering statistics from simulations with worldwide seismicity. The figures show the rate of occurrence of all possible earthquake pairs, $M \geq 6$, by the time intervals separating the pairs for different distance intervals. The rate of occurrence is normalized, such that purely random occurrence, without clustering, would have a normalized rate = 1.0.

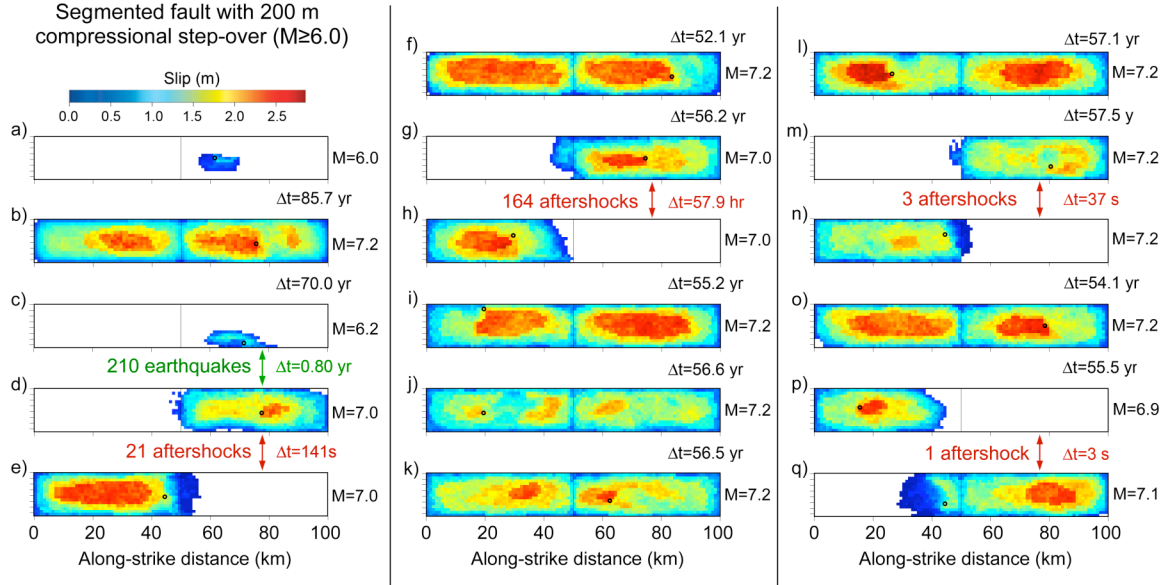


Figure 3. Model of two planar strike-slip fault segments, separated by a compressional step-over of 200m. Each fault segment is 50 km x 15km and is made up of 1 km² elements. The entire simulation consisted of 50,000 events. All $M \geq 6$ events in the simulation are shown in sequence (designated by letters a – q). Δt is the time interval between the $M \geq 6$ earthquakes.

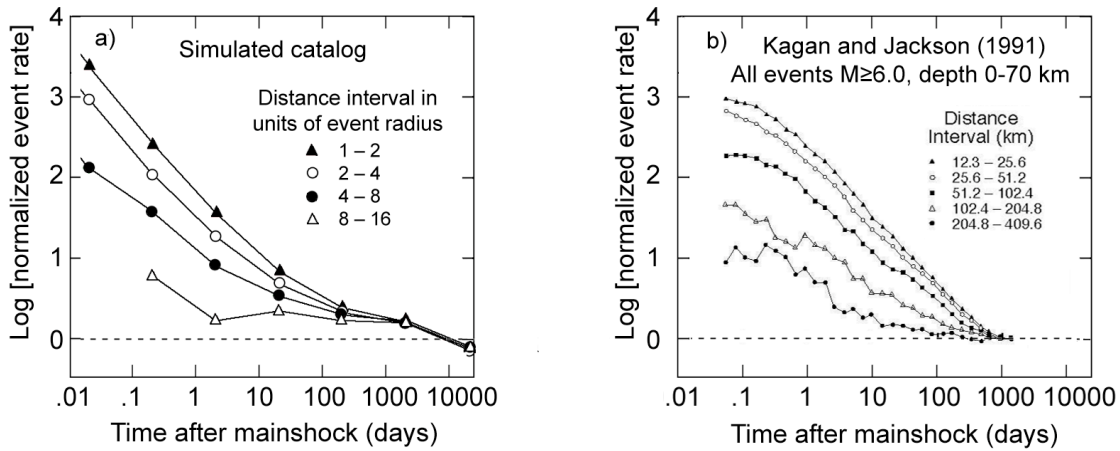


Figure 4. Normalized occurrence rate of all possible earthquake pairs, by the time interval between pairs and separation distance. For purely random occurrence, as described by a Poisson process, the logarithm of the normalized rate = 0 (normalized rate = 1) independent of separation distance. Clustering in these plots is due to Omori-law clustering with a characteristic fall-off with the separation distance. The principal effect is due to aftershocks with lesser contribution from foreshocks. a) Data from simulated catalog with 50,000 events. B) Harvard catalog data replotted from Kagan and Jackson (1991).

Future Directions

We anticipate productive use of this model to investigate a variety of topics pertaining to the physics of earthquakes occurring in complex fault systems. The capability to generate large numbers of events over a wide range of magnitudes, together with the incorporation of physical models of clustering processes, opens a variety of avenues for direct comparisons with earthquake catalogs. We believe the model will be an effective tool for simulating earthquakes and deformation in specific regional fault systems, and will find applications in estimation of regional earthquake probabilities.

References

Dieterich, J.H., 1992, Earthquake nucleation on faults with rate- and state-dependent friction, *Tectonophysics*, 211, 115-134.

Dieterich, J.H., 1995, Earthquake Simulations with Time-Dependent Nucleation and Long-Range Interactions, *Journal of Nonlinear Processes in Geophysics*, 2, 109-120.

Kagan, Y.Y., and D.D. Jackson, 1991, Long-term earthquake clustering, *Geophys. J. Int.*, 104, 117-133.

Okada, Y., 1992. Internal deformation due to shear and tensile faults in a half space, *Bull. seism. Soc. Am.*, 82, 1018-1040.